Gondwana Research 36 (2016) 14–27

Contents lists available at ScienceDirect

Gondwana Research

journal homepage: www.elsevier.com/locate/gr

Density structure of the cratonic mantle in Southern Africa: 2. Correlations with kimberlite distribution, seismic velocities, and Moho sharpness

Irina M. Artemieva [a,*], Lev P. Vinnik [a,b]

[a] Geology Section, IGN, University of Copenhagen, Copenhagen, Denmark
[b] Institute of Physics of the Earth, Moscow, Russia

ARTICLE INFO

Article history:
Received 26 July 2015
Received in revised form 1 May 2016
Accepted 7 May 2016
Available online 13 May 2016

Handling Editor: M. Santosh

Keywords:
Cratonic lithosphere
Mantle depletion
Metasomatism
Kimberlites
Diamond exploration

ABSTRACT

We present a new regional model for the depth-averaged density structure of the cratonic lithospheric mantle in southern Africa constrained on a 30′ × 30′ grid and discuss it in relation to regional seismic models for the crust and upper mantle, geochemical data on kimberlite-hosted mantle xenoliths, and data on kimberlite ages and distribution. Our calculations of mantle density are based on free-board constraints, account for mantle contribution to surface topography of ca. 0.5–1.0 km, and have uncertainty ranging from ca. 0.01 g/cm^3 for the Archean terrains to ca. 0.03 g/cm^3 for the adjacent fold belts. We demonstrate that in southern Africa, the lithospheric mantle has a general trend in mantle density increase from Archean to younger lithospheric terranes. Density of the Kaapvaal mantle is typically cratonic, with a subtle difference between the eastern, more depleted, (3.31–3.33 g/cm^3) and the western (3.32–3.34 g/cm^3) blocks. The Witwatersrand basin and the Bushveld Intrusion Complex appear as distinct blocks with an increased mantle density (3.34–3.35 g/cm^3) with values typical of Proterozoic rather than Archean mantle. We attribute a significantly increased mantle density in these tectonic units and beneath the Archean Limpopo belt (3.34–3.37 g/cm^3) to melt-metasomatism with an addition of a basaltic component. The Proterozoic Kheis, Okwa, and Namaqua–Natal belts and the Western Cape Fold Belt with the late Proterozoic basement have an overall fertile mantle (ca. 3.37 g/cm^3) with local (100–300 km across) low-density (down to 3.34 g/cm^3) and high-density (up to 3.41 g/cm^3) anomalies. High (3.40–3.42 g/cm^3) mantle densities beneath the Eastern Cape Fold belt require the presence of a significant amount of eclogite in the mantle, such as associated with subducted oceanic slabs.

We find a strong correlation between the calculated density of the lithospheric mantle, the crustal structure, the spatial pattern of kimberlites, and their emplacement ages. (1) Blocks with the lowest values of mantle density (ca. 3.30 g/cm^3) are not sampled by kimberlites and may represent the "pristine" Archean mantle. (2) Young (<90 Ma) Group I kimberlites sample mantle with higher density (3.35 ± 0.03 g/cm^3) than the older Group II kimberlites (3.33 ± 0.01 g/cm^3), but the results may be biased by incomplete information on kimberlite ages. (3) Diamondiferous kimberlites are characteristic of regions with a low-density cratonic mantle (3.32–3.35 g/cm^3), while non-diamondiferous kimberlites sample mantle with a broad range of density values. (4) Kimberlite-rich regions have a strong seismic velocity contrast at the Moho, thin crust (35–40 km) and low-density (3.32–3.33 g/cm^3) mantle, while kimberlite-poor regions have a transitional Moho, thick crust (40–50 km), and denser mantle (3.34–3.36 g/cm^3). We explain this pattern by a lithosphere-scale (presumably, pre-kimberlite) magmatic event in kimberlite-poor regions, which affected the Moho sharpness and the crustal thickness through magmatic underplating and modified the composition and rheology of the lithospheric mantle to make it unfavorable for consequent kimberlite eruptions. (5) Density anomalies in the lithospheric mantle show inverse correlation with seismic Vp, Vs velocities at 100–150 km depth. However, this correlation is weaker than reported in experimental studies and indicates that density-velocity relationship in the cratonic mantle is strongly non-unique.

1. Introduction

It has long been recognized that the structure of the continental lithosphere controls the emplacement of kimberlitic, particularly, diamondiferous magmatism; however, diamond prospecting is still subject to numerous uncertainties and unknowns. The importance of lithospheric age in diamond exploration has been recognized 50 years ago (Clifford, 1966). This observation that diamonds usually occur in crustal provinces older than 1.5 Ga has been adopted for many decades as a guiding principle of diamond exploration, known as the Clifford's Rule. Later modification to this rule (Janse, 1991) suggests that

* Corresponding author.
E-mail addresses: irina@ign.ku.dk (I.M. Artemieva), vinnik@ifz.ru (L.P. Vinnik).

http://dx.doi.org/10.1016/j.gr.2016.05.002
1342-937X/

diamonds are found only within lithosphere provinces older than 2.5 Ga. This conclusion has been challenged in some recent studies which suggest that few diamondiferous kimberlite pipes in North America (the Sloan and Argyle pipes) and Siberia (the Daldyn kimberlite province) may have been emplaced within the Proterozoic lithosphere (e.g. Carlson et al., 2004; Ionov et al., 2015). The evidence is, however, controversial since geochemical studies indicate that diamonds could have been derived from Archean lithosphere which underlies Proterozoic provinces (Schultze et al., 2008). In support of the Clifford's rule, petrological studies of xenolith-hosted mantle-derived peridotites have recognized significant variations in the composition of the continental lithospheric mantle, which are globally well correlated with the lithosphere age (e.g. Gaul et al., 2000). Intensive geochemical studies of mantle-derived rocks have established the existence of prominent differences between the composition of the cratonic Archean mantle and any other type of continental or oceanic lithosphere mantle (Boyd, 1989). However, it was recognized much earlier that Ca harzburgites are the distinctive component of cratonic lithospheric mantle, and that low-Ca harzburgites are characteristic of peridotite xenoliths from diamondiferous kimberlite pipes within Archean cratons (Sobolev, 1974; Gurney, 1984).

At about the same time, experimental studies of the graphite–diamond transition have established the temperature-depth stability field for diamond (Kennedy and Kennedy, 1976). This study provided the foundation for geophysical studies of the cratonic lithosphere in relation to diamond exploration (Snyder et al., 2004; Jones et al., 2009). Lithospheric keels which extend below the depth of the graphite–diamond transition are likely to be diamond rich; low lithospheric temperatures are a pre-requisite (Artemieva and Mooney, 2001).

A number of parameters measured in geophysical remote sensing experiments are highly sensitive to temperature, e.g. electrical conductivity and seismic velocities (e.g. Christensen, 1979; Shankland and Duba, 1990). In particular, the thickness of the electrically resistive lithosphere is strongly correlated with surface heat flow and therefore mantle temperatures (Artemieva, 2006). Interpretations of data from the Southern African Magnetotelluric Experiment (SAMTEX) have been used to establish correlations between the locations of diamondiferous kimberlites, mantle resistivity, and seismic velocity anomalies (Jones et al., 2009); however, these correlations are strongly non-unique.

Numerous seismic tomography studies have demonstrated that cratonic lithosphere is marked by high-velocity anomalies (e.g. Nataf and Ricard, 1996; James et al., 2001; Snyder et al., 2004; Lebedev et al., 2009; Saygin and Kennett, 2010; Lekic and Romanowicz, 2011; Kennett and Furumura, 2016), which to a large extent are caused by low temperatures in the cratonic lithosphere. However, compositional anomalies in the lithospheric mantle also produce variations in seismic velocities (Lee, 2003; Kopylova et al., 2004), such as increased SPT (at standard P–T, i.e. at Earth's surface) Vs velocities characteristic of kimberlite provinces (Artemieva, 2009).The lack of correlation between geoid anomalies and cratons with a high-velocity lithospheric mantle came as a surprise, as cold thick cratonic lithosphere was expected to be heavy (Jordan, 1975). This observation gave rise to the tectosphere hypothesis, according to which a density increase due to low temperature is nearly ideally compensated by a density decrease due to the unusual composition of the cratonic lithosphere (the isopycnic hypothesis) (Jordan, 1975, 1978). In particular, low-Ca harzburgites characteristic of the Archean mantle are important in producing low mantle density. Thus, geochemical and geophysical observations fit each other.

Gravity studies of density anomalies in the continental lithospheric mantle have demonstrated that the cratonic lithosphere is, indeed, low density, when density anomalies are reduced to SPT (that is standard, laboratory P–T) conditions (Kaban et al., 2003). High-resolution regional studies indicate, however, the presence of significant lateral density variations within the cratonic mantle of Europe (Artemieva, 2007), Siberia (Cherepanova and Artemieva, 2015), and southern Africa (Artemieva and Vinnik, 2016), and suggest that the isopycnic condition is satisfied mostly locally.

2. Modeling mantle density structure

A new regional model of density structure of the lithospheric mantle in southern Africa (Fig. 2) demonstrates strong density heterogeneity of the cratonic lithospheric mantle both at in situ and SPT conditions, even within lithospheric mantle of similar ages. The model is described in the companion paper (Artemieva and Vinnik, 2016), and the reader is referred to this publication for further details on the calculations procedure and the analysis of model uncertainties. The calculations are based on freeboard isostatic modeling with account for mantle contribution to an unusually high topography in Southern Africa. We have earlier applied the same approach to other cratons (Artemieva, 2003), and for Siberia we have tested the results of free-board modeling of mantle density anomalies (Cherepanova and Artemieva, 2015) towards gravity modeling (Herceg et al., 2016), demonstrating that the results of the two independent approaches not only provide similar values of lithosphere mantle densities but are also consistent with petrological data for mantle-derived peridotites from the Siberian craton.

For the cratons of southern Africa, the modeling results were calibrated by regional petrological data on mantle densities (e.g. O'Reilly and Griffin, 2006), which allowed for estimating mantle contribution to the southern Africa topography as ca. 0.5–1.0 km. Crustal contribution to the topography is calculated based on a regional receiver function analysis of the SASE (the Southern African Seismic Experiment) data on the Moho depth with regionally variable Vp/Vs ratio (Youssof et al., 2013). Despite the presence of strong compositional heterogeneity in the crust of southern Africa as indicated by the receiver function analysis, a constant value of average crustal density (2.85 g/cm^3 at room conditions) has been adopted in the absence of a unique correlation between Vp/Vs ration and density (Brocker, 2005). Lack of correlation between the calculated mantle density for the entire region and the crustal Vp/Vs ratio as determined from receiver function interpretations (Youssof et al., 2013) suggests that there are no systematic links between the density anomalies within the crust and the lithospheric mantle (Artemieva and Vinnik, 2016). Therefore, the assumption on the constant crustal density does not introduce any systematic bias into the final results. However, it produces some errors which cannot be assessed due to the absence of direct information on the crustal density structure. Crustal contribution to density uncertainty seems to be crucial only for the East Cape Fold belt (Fig. 2) where receiver function analysis indicates extreme values of both the Moho depth and Vp/Vs ratio (Youssof et al., 2013).

Information on crustal structure and mantle contribution to the topography allows for calculating density structure of the lithospheric mantle by assuming that the isostatic compensation is achieved at the base of the lithosphere. An introduction of temperature-correction to calculated in situ mantle densities allows for calculating mantle densities at SPT conditions and therefore for their comparison with petrological data. For consistency of the calculations, the depth to the lithosphere base and lithospheric geotherms are based on thermal modeling constrained by borehole heat flow measurements and further calibrated by regional xenolith P–T arrays. The analysis of uncertainties in the calculated density structure of the lithospheric mantle includes uncertainties associated with the unknown density of the crust, uncertainties in lithosphere thickness, and the value of sublithospheric mantle contribution to surface topography. The analysis of the possible parameter space indicates that the largest uncertainty is associated with the value of mantle (dynamic) contribution to the topography, which is between 0.5 km and 1 km. This uncertainty transfers to the uncertainty of lithosphere mantle density which ranges from ca. 0.01 g/cm^3 for the Archean terrains to ca. 0.03 g/cm^3 for the Namaqua–Natal and Cape Fold belts (Fig. S1 in the online version at http://dx.doi.org/10.1016/j.gr.2016.05.002.).

In the present study, we compare our recent model of the mantle density structure of the Kalahari craton (Fig. 2) with petrological data on xenolith-derived mantle peridotites and with regional seismic models of the lithosphere. These independent data allow us to examine the links between mantle density, tectonic evolution, Moho sharpness, and seismic Vp, Vs in the mantle. We further analyze correlations between mantle density and the distribution of diamondiferous and non-diamondiferous kimberlites (Fig. 3 and Section 5), thus proposing a new strategy for diamond prospecting.

3. Mantle density versus lithosphere age

Synthetic density calculations from mineral compositions constrained by xenolith samples (Gaul et al., 2000; Poudjom Djomani et al., 2001) indicate a pronounced age-dependence of density of the cratonic mantle (Fig. 4a). We use our regional new model of lithosphere mantle (LM) density (Fig. 2) to examine correlations between density of the subcontinental lithosphere mantle and the lithosphere age in different tectonic provinces of southern Africa (Fig. 4b).

3.1. Blocks where mantle density follows a global petrological pattern of age-dependence

In general agreement with petrological data, mantle density structure in southern Africa shows an overall trend in a gradual density decrease from the Cenozoic Cape Fold belt to the Proterozoic Okwa and Kheis blocks and to the Archean Kaapvaal craton (Carlson et al., 2005). The range of density values reported in petrological studies for the lithospheric mantle of different ages (e.g. Boyd, 1989; Hawkesworth et al., 1990; Pearson et al., 1995; Jordan, 1988; *Poudjom Djomani et al.*, 2001; *James et al.*, 2004; O'Reilly and Griffin, 2006) (Fig. 4a) corresponds to the range of mantle density values calculated by free-board modeling (Artemieva and Vinnik, 2016). Further details on the calculation method and on the mantle density structure in southern Africa may be found in this companion paper.

3.1.1. Cape Fold belt (ca. 280 Ma)

Two provinces of the Cape Fold belt, Eastern and Western, have a significantly different tectonic evolution and also have prominent differences in mantle density structure. The Eastern Cape Fold belt (ca. 280 Ma) has a high-density mantle (3.46–3.50 g/cm^3), which may, however, be an artifact of the crustal model used in the calculations (see Section 2). If real, this high-density anomaly would require the presence of a significant amount of eclogite in the mantle. In the Western Cape Fold Belt, the lithospheric mantle is weakly depleted with SPT density typically of 3.37–3.38 g/cm^3. This province has Precambrian (1.2–0.5 Ga) basement which was intruded by late Precambrian Cape granites during the Saldanian (Pan-African) orogeny. The Western and Eastern Cape provinces are separated by a belt of low-density mantle (3.33–3.35 g/cm^3), with density values similar to the Kaapvaal craton (Fig. 4b). Intriguingly, the only kimberlite pipe within the Cape Fold belt which is included into the global kimberlite database (Faure, 2006) is located exactly within the strongly depleted lithosphere belt (Fig. 2a). This observation provides a strong support to the resolution of our mantle density model.

3.1.2. Proterozoic mobile belts (1.1–2.0 Ga)

Similar to the Cape Fold Belt, the Kheis belt (1.7–2.0 Ga) has two parts (Fig. 2a), with fertile mantle (SPT density of ca. 3.37–3.41 g/cm^3) in the southern part where no kimberlites are known and a low-density (3.32 g/cm^3) highly depleted lithospheric mantle in the northern part. Intriguingly, kimberlites follow the edges of the low-density mantle block in the central part of the Kheis belt, but none are located within it (Fig. 2a).

In the Namaqua–Natal mobile belt (1.1–1.3 Ga), the density structure of the lithosphere mantle is heterogeneous, with an overall fertile composition (3.37–3.41 g/cm^3) and higher densities (3.40–3.41 g/cm^3) in the western part where kimberlite pipes are absent (Fig. 2b). Most kimberlite pipes within the Namaqua–Natal belt are in its central part and follow a narrow belt of a relatively low-density mantle (3.34–3.36 g/cm^3). In agreement with our results, which show the presence of a fertile mantle with density of 3.40–3.41 g/cm^3 in the western part of the Namaqua–Natal mobile belt, the global kimberlite database (Faure, 2006) does not list any kimberlite pipes in this area (Fig. 2a).

3.1.3. Kaapvaal and Zimbabwe cratons (3.2–3.7 Ga)

Lithosphere mantle density in the Kaapvaal craton (3.2–3.7 Ga) indicates a strongly depleted mantle, with only a very weak difference between the western and eastern blocks (3.32–3.34 g/cm^3 and 3.31–3.33 g/cm^3, respectively). Except for Lesotho, regions with the most depleted mantle (3.30–3.32 g/cm^3) in the Kaapvaal craton are not sampled by kimberlites (Fig. 2a). The region with a high density of kimberlite pipes follows the belt of a slightly increased mantle density (ca. 3.33 g/cm^3) as compared to less dense and more depleted mantle to the east and to the west (Fig. 2a). Note that the results for Lesotho should be treated with caution: this region has extremely high topography (2.5 km) and strong positive free air anomalies (+100 + 150 mGal), indicating that it is not isostatically compensated as assumed in free-board modeling.

The Witwatersrand Basin (2.05 Ga) of the eastern Kaapvaal block is resolved as a block with a slightly increased mantle density. Similarly, the Bushveld Intrusion Complex (ca. 2.05 Ga) in the northern part of the Kaapvaal craton is clearly resolved as a coherent structure with an increased density (3.34–3.35 g/cm^3), which is typical of Proterozoic but not of Archean mantle (Fig. 4b). There is no difference between the western and eastern lobes of the Bushveld Complex and we attribute an increased mantle density to magmatic metasomatism at the time of its emplacement (Scoon, 1987; Mathez, 1995)), since an introduction of iron-rich basaltic magmas into cratonic mantle increases its density (Carlson et al., 1999; Irvine et al., 2001). The Pietersburg/Giyani terrain between the eastern lobe of the Bushveld complex and the Limpopo belt has a low density mantle (3.32–3.33 g/cm^3) and apparently represents a small block of preserved Kaapvaal mantle.

In most of the Zimbabwe craton (2.8–3.7 Ga), in particular in the eastern block, the lithospheric mantle has low density (3.32–3.33 g/cm^3, with −1.5% to −2% of density deficit) and is similar to the Kaapvaal craton. The Great dyke of Zimbabwe seems to mark the eastern edge of the most depleted mantle but it is not seen in mantle density structure, in agreement with geological evidence that this is a shallow crustal feature.

3.2. Deviations from the global petrological pattern of age-dependence of mantle density

There are a number of clear exceptions from the global petrological trend shown in Fig. 4a, with several tectonic blocks having a much denser lithospheric mantle than the trend suggests. They include the southern Kheis belt, the Limpopo belt, the Barberton greenstone belt/Swaziland, and the western part of the Zimbabwe craton (Fig 4b). We interpret the presence of atypical high-density material in the mantle of these blocks by metasomatism caused by an introduction of iron-rich basaltic melts into cratonic lithosphere (Bailey, 1982) during different magmatic episodes that took place over a long geodynamic evolution of the cratons of southern Africa (Fig. 1). Metasomatic modification of cratonic mantle through plate tectonics processes and by mantle convective instabilities is well documented by petrological studies worldwide (Coltorti and Gregoire, 2008) and therefore provides sound explanation for high-density anomalies in cratonic mantle, which otherwise is expected to have low density (Jordan, 1975, 1978; Carlson et al., 1999; Gaul et al., 2000; Poudjom Djomani et al., 2001) due to unique P–T conditions of its differentiation from the mantle (Walter, 1999, 2005).

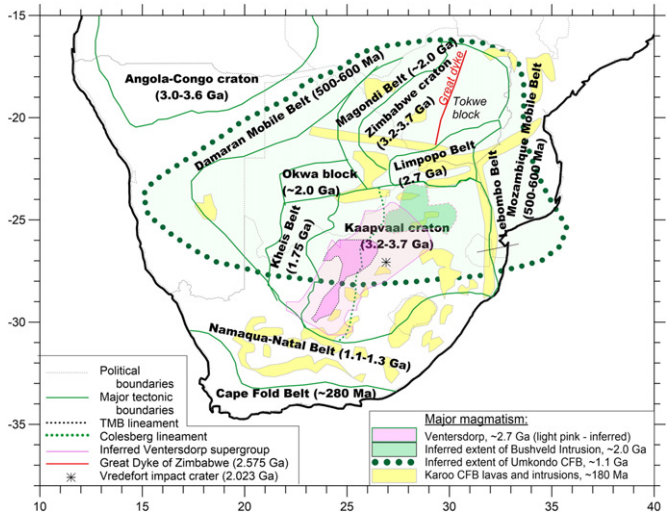

Fig. 1. Major tectonic provinces of southern Africa. Tectonic boundaries—after de Wit et al. (1992) and Goodwin (1996); the Neoarchean Ventersdorp magmatic province—after Schmitz and Bowring (2003), the inferred extent of the Bushveld Igneous Complex—after Campbell et al. (1983), and of the Umkondo continental flood basalt province (CFB)—after Hanson et al. (2004); major Karoo lavas and outcrops—after Riley et al. (2006).

3.2.1. Limpopo belt (2.7–3.0 Ga)

The Limpopo belt (2.7–3.0 Ga) represents a significantly reworked Archean mantle with an increased mantle density (3.34–3.37 g/cm^3) typical of metasomatized cratonic roots. The central part of the Limpopo belt, which is sampled by the Cambrian diamondiferous Venetia and River Ranch kimberlites (see Fig. 3b for location), has the least depleted mantle (3.37–3.38 g/cm^3). Petrological studies of mantle-derived peridotites from these two pipes (with Archean Re-depletion ages of ca. 3.0 Ga, Carlson et al., 1999) suggest that a highly depleted material is present in the bottom portion of the lithospheric mantle which may represent a southward continuation of the depleted Tokwe block of the Zimbabwe craton (Smith et al., 2009). Note that our model cannot constrain the depth distribution of density anomalies but provides an average density for the entire lithospheric mantle, further averaged for blocks ca. 50 × 50 km. It is worth noting that young kimberlites sample more depleted mantle within the western and eastern Limpopo (with LM density of ca. 3.35 g/cm^3), while the least depleted part of the belt (with LM density of ca. 3.37–3.38 g/cm^3) is around much older (Cambrian) and diamondiferous Venetia and River Ranch kimberlites (Figs. 2a, 3).

3.2.2. Zimbabwe craton (3.2–3.7 Ga)

In the western part of Zimbabwe craton (2.6–2.8 Ga), the lithosphere mantle is fertile, with density increase from 3.37 to 3.40 g/cm^3 towards the Magondi belt. This high-density anomaly may, at least in part, be an artifact of a strong anomaly in the crustal structure (Youssof et al., 2013) used to model mantle density.

Note that, except for the western Zimbabwe craton, three other tectonic blocks with denser than expected lithospheric mantle fall onto the line (marked as "metasomatic trend" in Fig. 4b) which is shifted by the same value (ca. 0.03 g/cm^3) from the global density-age trend. This observation may suggest that there may be a natural petrological limit to the extent of metasomatic enrichment of the cratonic mantle, beyond which it delaminates when the lithospheric density becomes too high. This may happen, for example, if a part of basaltic additions undergoes phase transformation to eclogite. A possibility of the presence of eclogitic material in some parts of the lithospheric mantle cannot be ruled out, and the presence of eclogite in lithospheric mantle is well documented for the South African, Siberian, West African, and Slave cratons (Neal et al., 1990; Jerde et al., 1993; Barth et al., 2001; Kopylova et al., 2016).

Here we want to note again that our results provide only the depth-averaged value of mantle density and the depth distribution of density anomalies in tectonic provinces that fall onto the proposed "metasomatic trend" may be significantly different. In particular, studies of mantle xenoliths from the southwestern Kaapvaal craton (Group I, emplacement age < 90 Ma) demonstrate a complicated pattern of density variations with depth (James et al., 2004; O'Reilly and Griffin, 2006). These data also suggest a significantly denser lithospheric mantle of the Kaapvaal craton (with a depth-average value of ca. 3.35–3.36 g/cm^3 between 80 and 160 km depth in kimberlite pipes) than does the free-board calculation (3.32–3.33 g/cm^3 averaged for the depth range from the Moho (ca. 35–40 km) to the LAB (ca. 180–220 km) and averaged laterally over 50 × 50 km).

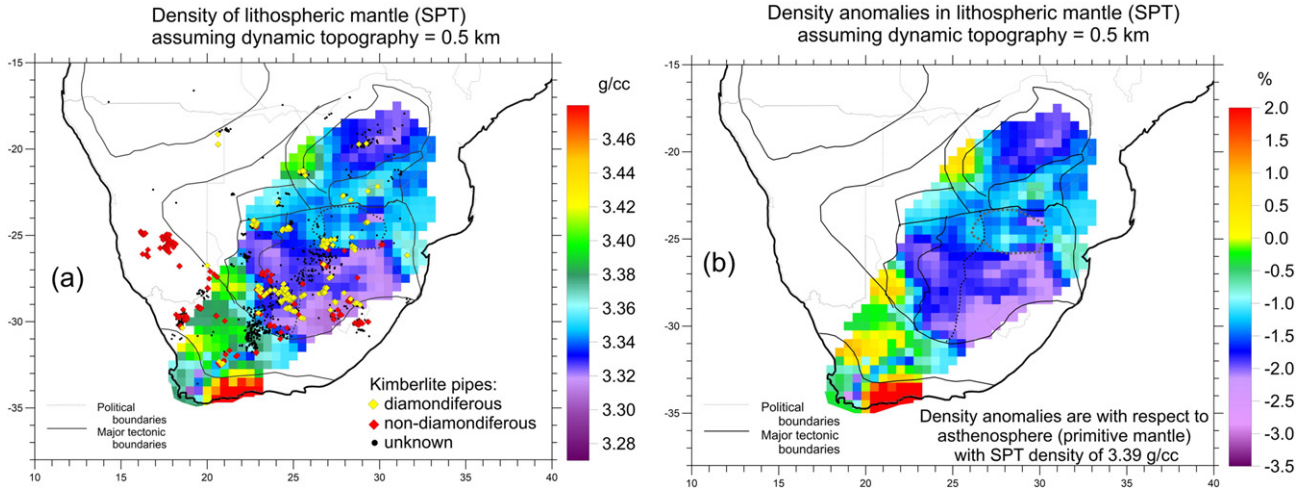

Fig. 2. Density of lithospheric mantle at SPT conditions (at Earth's surface): (a) absolute values, (b) density anomaly with respect to convective mantle with density of 3.39 g/cm^3. The maps are calculated assuming mantle dynamic (or residual) contribution to topography is 0.5 km (Artemieva and Vinnik, 2016). The uncertainty associated with the value of mantle dynamic topography is ca. 0.01 g/cm^3 for most of the Archean blocks and increases to ca. 0.02–0.03 g/cm^3 in the Cape Fold and Namaqua–Natal belts (Fig. S1 in the online version at http://dx.doi.org/10.1016/j.gr.2016.05.002.). Very high-density anomaly in the Eastern Cape Fold belt is likely to be artifact which propagates from the anomaly in the crustal model (deep Moho (47–48 km) and low Vp/Vs = 1.6 (Youssof et al., 2013)). SPT density values may be directly compared to petrological data, having in mind that they correspond to vertically averaged mantle density in the layer between the Moho and the LAB.

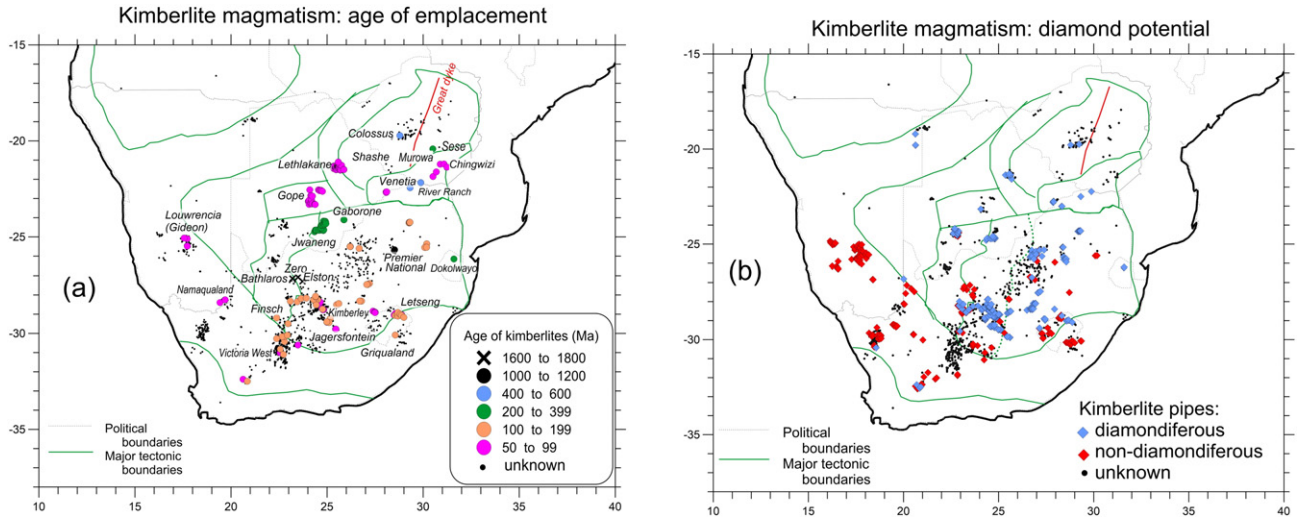

Fig. 3. Distribution of kimberlite magmatism in southern Africa (based on database of Faure, 2006). (a) Symbols—kimberlite pipes shown by the age of emplacement; (b) diamond potential; the names of some kimberlite pipes are shown in italics. Note that for a large number of kimberlite pipes information on kimberlite ages and diamond potential is not publically available.

Importantly, only few regions have mantle density slightly lower than suggested by global petrological data. This includes parts of the northern Kheis belt and the Western Cape Fold belt (Fig. 4b). A possible interpretation is that the basement age in these provinces may be older than dated at present, e.g. they may be underlain by an older lithosphere.

4. Mantle density, isopycnicity, and xenolith data

4.1. Testing isopycnicity

The isopycnic hypothesis has been seriously questioned in a series of recent studies (Kelly et al., 2003; Eaton and Perry, 2013; Cherepanova and Artemieva, 2015). In case of isopycnic lithosphere (and with no consideration if the isopycnic condition is satisfied at any depth or for the bulk mantle), average bulk density of the lithospheric mantle at in situ conditions (Fig. 5a) should be close to in situ density of asthenosphere (3.235 g/cm^3) and be the same throughout the entire region.

Our results indicate that isopycnicity may not be entirely satisfied in southern Africa (Fig. 5b). However, for most of the Archean part of southern Africa deviations of bulk mantle density from the bulk isopycnicity are small and within the range of 0.01–0.02 g/cm^3 (Fig. 5b), which is close to model uncertainty. Note that most kimberlite pipes from the Kaapvaal craton which have been studied in the public domain are restricted to the region with near-zero or small deviations from isopycnicity. In contrast, the isopycnic condition is clearly not satisfied in the Proterozoic–Phanerozoic block in the southern part of the region, as well as in the Limpopo Belt and along the eastern margin of the Kaapvaal craton.

4.2. Bulk mantle Mg# versus Mg# in olivine

A number of petrological studies of mantle-derived xenoliths from southern Africa focus on density structure of the lithospheric mantle (e.g. James et al., 2004; Kuskov et al., 2006). Most of the petrological data are from the Kimberley province in the south-western part of the Kaapvaal craton, where numerous kimberlites of Group I (<90 Ma) have been studied. Based on these data and assuming the "ideal isopycnicity" satisfied at any depth within the lithospheric mantle, Jordan (1988) has proposed a linear relation between mantle density

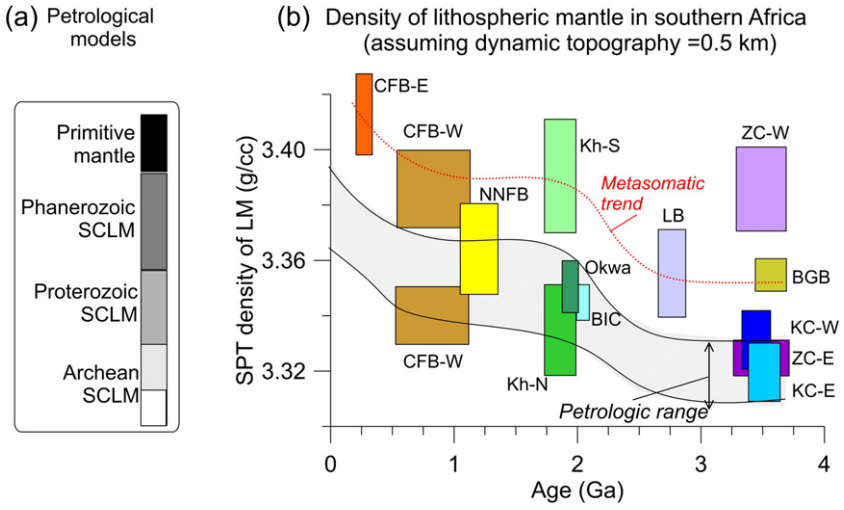

Fig. 4. Density structure of the subcontinental lithospheric mantle (SCLM) at SPT conditions as a function of age: (a) worldwide based on petrological studies; (b) in different tectonic provinces of southern Africa based on the present study (Fig. 2a). Vertical size of boxes shows the average value with standard deviation, horizontal size shows the time span for the lithosphere age. The density range shown in (a) is marked in (b) by two solid lines; red line marks the proposed metasomatic trend. Abbreviations: CFB-E and CFB-W—Eastern and Western Cape Fold belt; NNFB—Namaqua–Natal Fold belt; Kh–S and Kh–N—southern and northern Kheis belt; BIC—Bushveld intrusive complex; LB—Limpopo belt; ZC-W and ZC-E—western and eastern (Tokwe block) Zimbabwe craton; KC–W and KC–E—western and eastern Kaapvaal craton; BGB—Barberton greenstone belt.

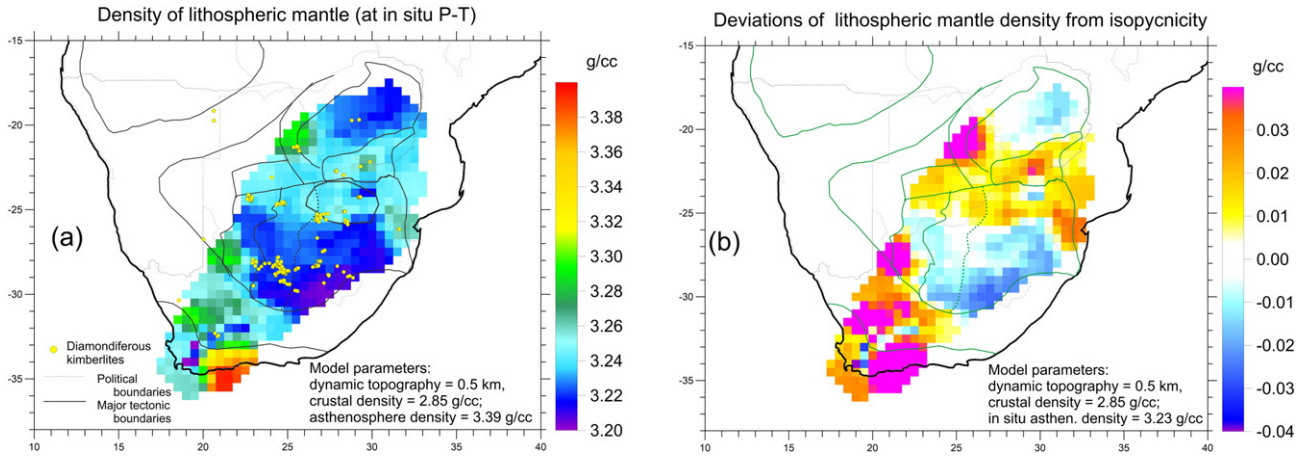

Fig. 5. (a) Density of lithospheric mantle at in situ conditions (assuming mantle dynamic contribution to topography is 0.5 km (Artemieva and Vinnik, 2016)). These density values may be directly compared to geophysical remote sensing models (e.g. seismic and gravity). (b) Deviation of lithospheric mantle from isopycnicity (the map shows the difference between (a) and 3.23 g/cm^3). In case the isopycnic condition is satisfied, average bulk density of the lithospheric mantle at in situ conditions should be close to in situ density of asthenosphere (3.23 g/cm^3). In Kaapvaal, isopycnicity is best satisfied around the best studied kimberlite clusters.

(in g/cm^3) and Mg# [Mg# = (5.093-density)/0.0191]. Another relation, which links bulk peridotite density to Mg# (Mg/Mg + Fe) in olivine, has been proposed by *Lee* (2003) based on synthetic calculations of density of cratonic peridotite from known mineralogy [Mg#(ol) = (4.74-density)/0.0152]. We used these relations to calculate mantle Mg# from mantle density.

Assuming isopycnicity is nearly satisfied in southern Africa (at least in the Archean blocks), we convert SPT density of the lithospheric mantle (Fig. 2a) to Mg# (Fig. 6ab) using the linear correlation between the two parameters (Jordan, 1988; Lee, 2003). We next compare synthetic Mg# with mantle Mg# in olivine (Griffin et al., 2003; Smith et al., 2009) (Fig. 6b). Strictly speaking, the comparison is not adequate because synthetic Mg# calculated from mantle density refers to the bulk composition of the lithospheric mantle, while petrologic Mg# refers to olivine, that is to ca. 65–70% of composition of the lithospheric mantle (Fig. 7 in Artemieva and Vinnik, 2016). The presence of even a small amount of garnet in mantle peridotite will significantly increase mantle density, while the presence of a significant amount of clinopyroxene and orthopyroxene will decrease it (Jordan, 1979).

For the Archean terranes of southern Africa, our calculations suggest higher variability in bulk mantle Mg# than indicated by xenolith studies for Mg# in olivine (Fig. 6b). Both geophysical and petrological models indicate high Mg# in the lithospheric mantle of the Kaapvaal and Zimbabwe cratons; for these cratons, the two approaches are in overall agreement with Mg# of ca. 92.5–93.5. In regions with no kimberlite sampling, synthetic Mg# calculated from mantle density anomalies are slightly higher (ca. 94–95) than the maximal reported petrological Mg#.

Petrological studies of xenoliths from the Murowa and Sese kimberlites of the Tokwe block in the southern Zimbabwe craton indicate extremely depleted mantle with Mg# of up to 95 (Smith et al., 2009). This is consistent with the results of the present study, which also demonstrate that the lithospheric mantle in the eastern Zimbabwe craton may be strongly depleted (Mg# ~ 93). However, due to vertical averaging of density structure and lateral averaging over 30′ × 30′ cells, the strongest density anomalies seen in "point" xenolith data will inevitably become smeared in our geophysical model.

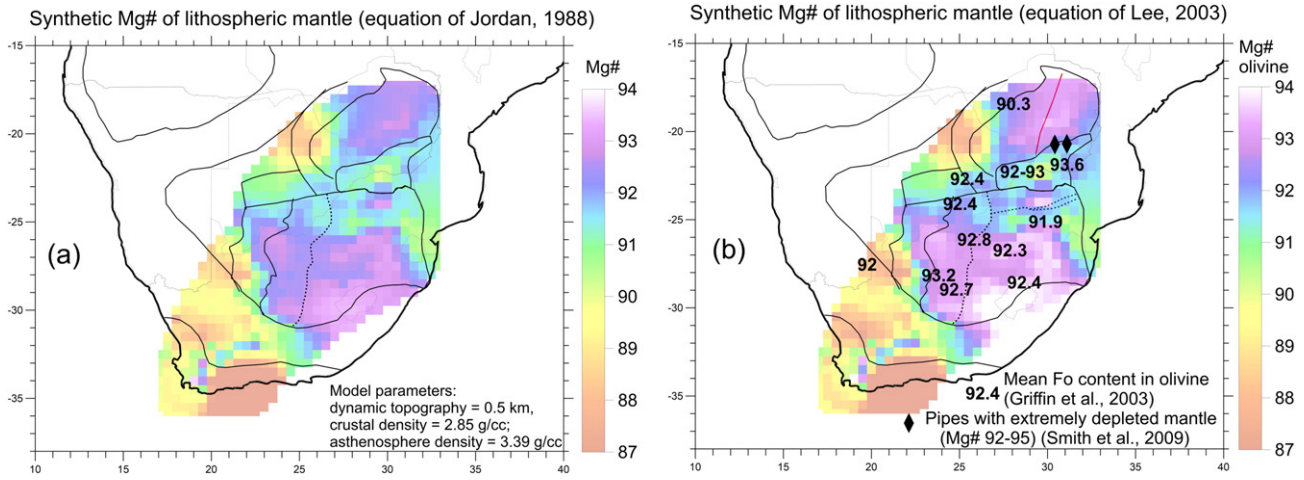

Fig. 6. Synthetic bulk Mg# calculated from SPT mantle density (Fig. 2a): (a) Mg# for bulk composition based on the isopycnic equation of Jordan (1988); (b) Mg# in olivine based on equation of Lee (2003); numbers—petrologic data on mantle Mg# calculated as mean Fo content in olivine (Griffin et al., 2003) and as Mg# in olivine (Smith et al., 2009). In places where the isopycnic condition is not fully satisfied (Fig. 5b), the conversion of mantle density to Mg# is, strictly speaking, inaccurate. Note that synthetic values of Mg# correspond to vertically averaged structure of subcrustal lithosphere (from the Moho to the LAB), which may be different from depth averaging of petrological data shown in (b).

There is a significant discrepancy between Mg# calculated from petrological and geophysical data for the Limpopo belt. A petrological study of mantle-derived peridotites in southern Africa (Griffin et al., 2003) reports the most depleted mantle to be beneath the Limpopo belt. Xenolith studies of the Cambrian Venetia (Stiefenhofer et al., 1999) and River Ranch (Kopylova et al., 1997) kimberlites provide Mg# in olivine of up to 94 and 92–93, correspondingly. In contrast, our results suggest a significantly lower bulk mantle Mg# of ca. 90.5 for the Limpopo mantle around the Venetia and River Ranch pipes. A possible explanation is that xenolith-based Mg# corresponds to mantle composition prior and during kimberlite magmatism (>400 Ma ago), while "synthetic" geophysical Mg# corresponds to the present-day density structure of the mantle. In that case, a significant refertilization of the Limpopo mantle may have taken place during the Gondwana break-up (the Karoo event).

5. Mantle density and kimberlite distribution

5.1. Correlation with kimberlite ages

Our analysis of kimberlite distribution in relation to the density structure of the lithospheric mantle is based on publically available global kimberlite database (Faure, 2006). For the cratons of southern Africa, it includes ca. 1300 kimberlite pipes, with the ages available for only ca. 200 of them, and the information on diamond potential available for 405 pipes. Therefore, it is important to have in mind that our database of kimberlite ages and their diamond potential is extremely incomplete, and our conclusions may be significantly biased. With this limitations in mind, we make the following conclusions from the available data:

- concentration of kimberlite pipes is the highest in regions with low-density lithospheric mantle (Fig. 7a, 8a), and the peak concentration of kimberlites is in mantle blocks with average density of 3.32–3.33 g/cm^3 (Fig. 7b);
- young (<200 Ma) kimberlite magmatism apparently had a significantly weaker metasomatic impact on the cratonic mantle, given that numerous kimberlites sampling low-density cratonic nuclei are young (Fig. 7c);
- apparently the maximal density of the lithospheric mantle beneath the kimberlite provinces may be directly linked to the emplacement age of kimberlites (Fig. 7c).

These observations suggest that the present-day density structure of the cratonic mantle may reflect the degree of its metasomatic enrichment after (or during) the kimberlite emplacement (Cordier et al., 2015). If so, it is surprising because other magmatic events (e.g. the Bushveld intrusion or the Karoo traps) have also significantly affected composition of the cratonic mantle. Therefore, a direct comparison of geophysical models (which refer to the present-day mantle structure) with petrological models (which reflect mantle structure during

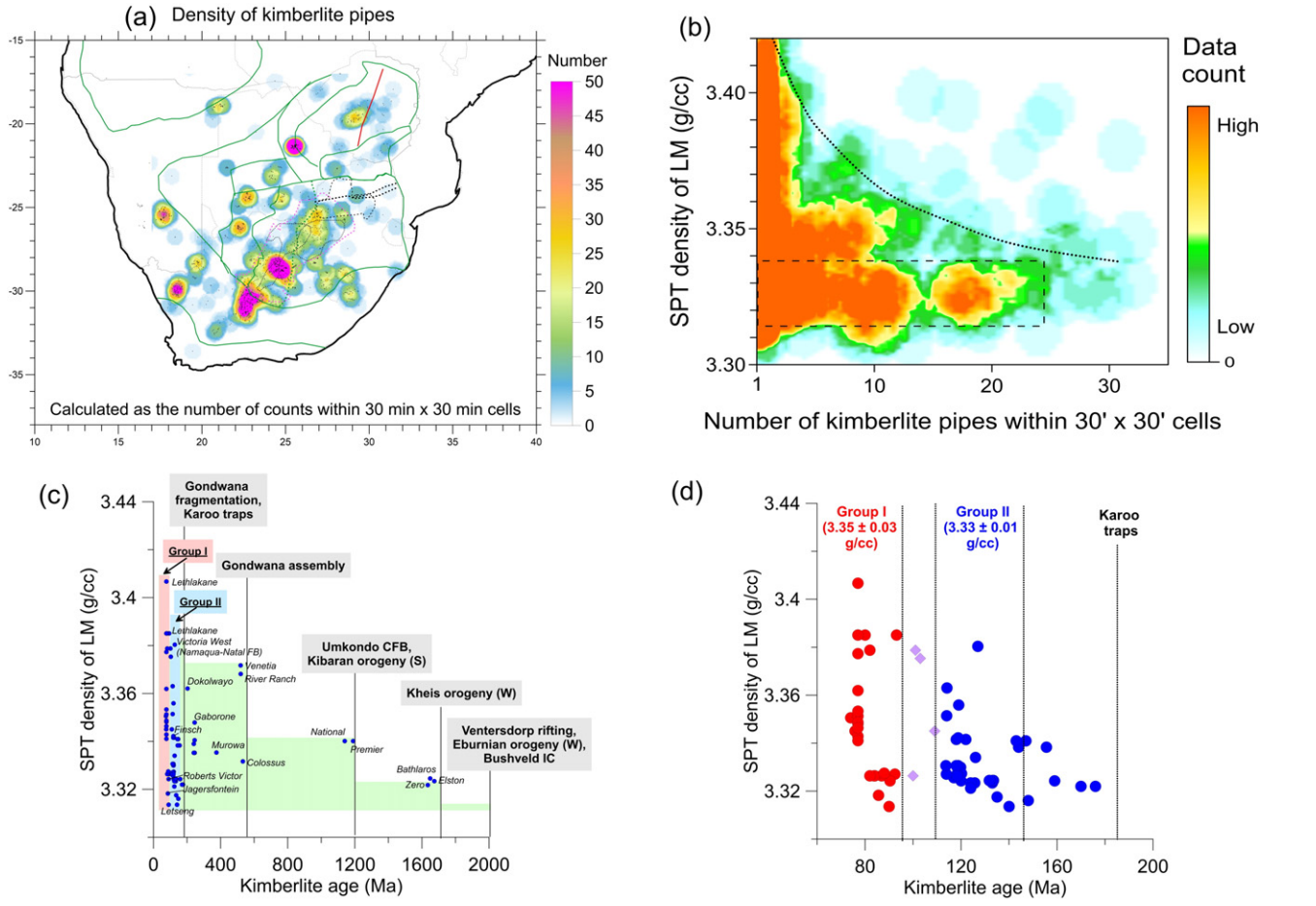

Fig. 7. Statistical analysis of distribution of kimberlite pipes. (a) Number of kimberlite pipes within 30 × 30 min cells; (b) density of kimberlite clusters as a function of SPT mantle density (Fig. 2a); (c) age of kimberlites as function of the present-day SPT density of the lithospheric mantle, zoomed at Cretaceous kimberlites (d). Kimberlites of Group I (with emplacement ages <95 Ma) sample mantle with higher density than Group II (>110 Ma) kimberlites (d). Statistics may be biased by incomplete information on kimberlite ages in the database (Faure, 2006). We propose a step-wise, spatially heterogeneous, increase in density of the Kaapvaal LM in response to large-scale tectono-magmatic events (c).

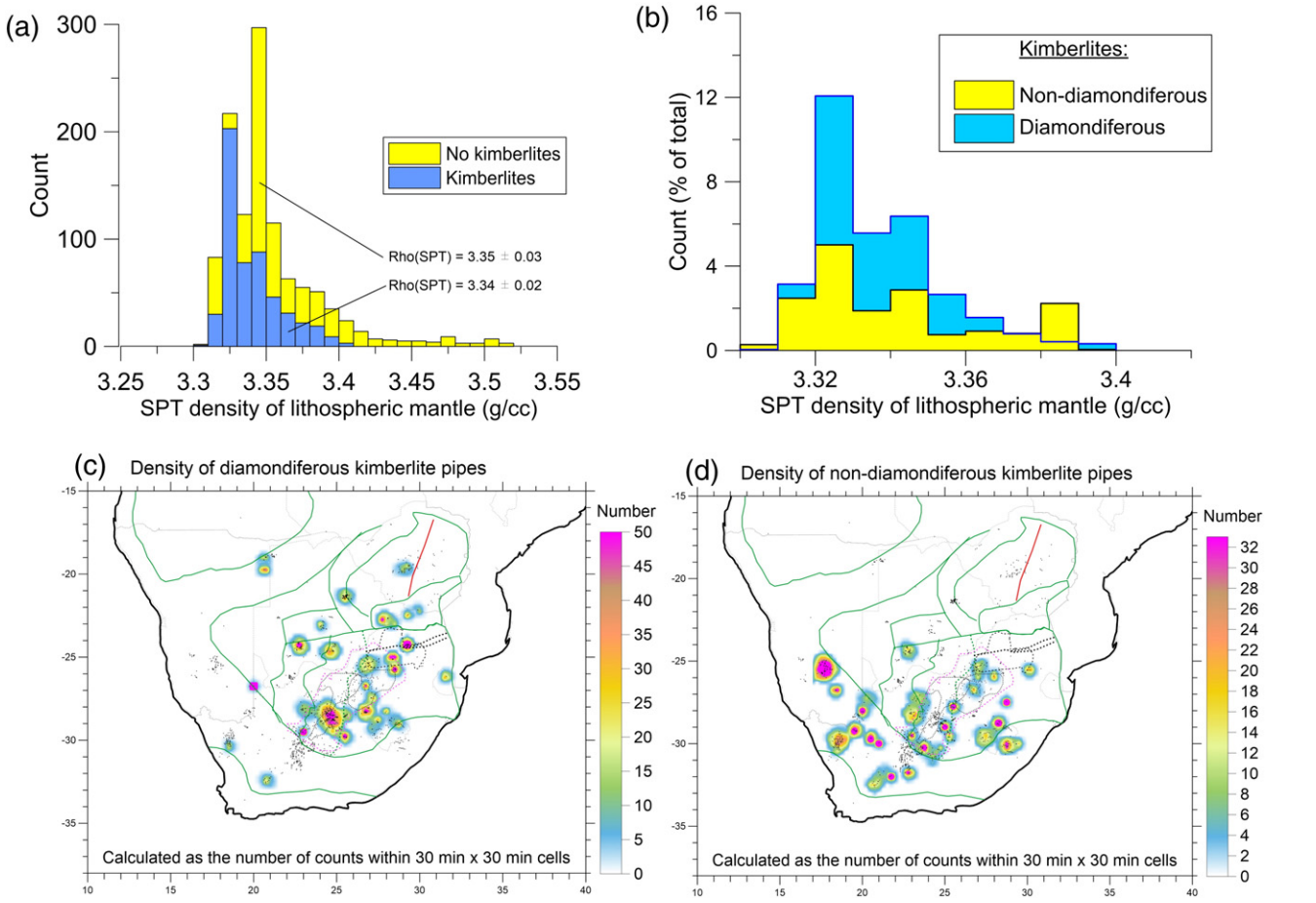

Fig. 8. Statistical analysis of distribution of diamondiferous and non-diamondiferous kimberlites (note that for a significant number of pipes, this information is not publically available). Histograms (calculated on a 15 × 15 min grid) of SPT density of the lithospheric mantle for regions (a) with and without kimberlites, (b) with and without diamondiferous kimberlites. (c, d) Number of diamondiferous and non-diamondiferous kimberlites within 30 × 30 min cells.

kimberlite emplacement) should be made with caution. As a consequence, knowledge on the present-day structure of the cratonic mantle is important (but insufficient on its own) for diamond prospecting.

5.2. Group I versus Group II kimberlites

Most kimberlites of southern Africa are Cretaceous (Fig. 7c). Historically, they have been subdivided into two distinct types, first by petrographic observations, and later by isotope compositions when the terms Group I and Group II kimberlites have been introduced (Smith, 1983). Young, Group I kimberlites, historically termed "basaltic," are CO_2-rich ultramafic potassic igneous rocks with the emplacement ages of <95 Ma. In contrast, older (>110 Ma) Group II kimberlites, are K-rich peralkaline rocks, which are also rich in water; it has been argued that their composition is closer to lamproites than to Group I kimberlites (Mitchell, 1995; Ulmer and Sweeney, 2002), and their origin is thought to be related to the Gondwana break-up.

Petrological data suggest that the older, Group II kimberlites, brought xenoliths from a more depleted mantle than the younger ones (Griffin et al., 2003). Although this conclusion is debated, our results (Fig. 7d) indicate that the Kaapvaal Group I and Group II kimberlites are emplaced in the lithospheric mantle with a significantly different density (3.35 ± 0.03 g/cm^3 and 3.33 ± 0.01 g/cm^3, respectively), with older kimberlites sampling a more depleted mantle. We speculate that progressive age-dependent differences in mantle density reflect metasomatic enrichment of cratonic mantle, and note the limitations of the kimberlite database which we use in the analysis.

5.3. Mantle density and diamondiferous kimberlites

A comparison of the present-day mantle density structure with the location of diamondiferous and non-diamondiferous kimberlites shows no simple pattern for the cratonic interior (Fig. 8 cd).

- In general, diamondiferous kimberlites are more numerous in regions with low-density cratonic mantle (3.32–3.35 g/cm^3), while non-diamondiferous kimberlites sample mantle with a broad range of density values.
- Most kimberlites in regions with high mantle density are non-diamondiferous. The only notable exception is the Lethlakane cluster at the western edge of the Zimbabwe craton (see Fig. 3a for location); however, the crustal structure in this region is not well constrained and the calculated high-density anomaly may be a model artifact due to incomplete crustal correction.
- In some places (e.g. the Premier pipe in the Bushveld Complex, several pipes of the Limpopo Belt (e.g. Venetia and River Ranch), Okwa block, and Swaziland), the diamondiferous kimberlites are located in regions with moderately depleted mantle (with mantle density of 3.35–3.37 g/cm^3). All such pipes seem to be older than 200 Ma (compare with Fig. 3, Fig. 7c). We interpret the present-day mantle density anomalies around these pipes to reflect intense reworking of the cratonic mantle by a younger (post-kimberlite) tectonism.
- Some non-diamondiferous kimberlites are present in regions with low-density, strongly depleted mantle. Many of such kimberlite clusters tend to be at the edges of the strongly depleted lithospheric blocks, along the south-western and eastern margins of the Kaapvaal

craton. We note that some kimberlite pipes do not host diamonds due to conditions of their emplacement (when diamonds "burned" to carbon during kimberlite eruption) rather than because they sampled non-diamondiferous mantle.

6. Moho sharpness, kimberlite occurrences, and mantle density

We next compare density structure of the lithospheric mantle with seismic models based on interpretations of the data from the SASE seismic experiment. This includes regional receiver function (RF) analysis of the Moho sharpness (Youssof et al., 2013) and mantle P- and S-wave velocities based on regional body-wave tomography (James et al., 2001; Youssof et al., 2015). Heterogeneity and complexity of the crust–mantle transition in southern Africa has been discussed in other papers (e.g. Nguuri et al., 2001; Niu and James, 2002; James et al., 2003), where a sharp Moho with a strong velocity contrast was found in crustal blocks undisturbed since the Archean, and a diffuse Moho was found in regions with modified crust and in post-Archean terranes. Unfortunately, a quantitative measure of the Moho sharpness is not available from these studies, thus making them unsuitable for our analysis. We also note that these receiver function interpretations assume a constant Vp/Vs ratio in the crust for all (e.g. Nguuri et al., 2001) or some of the stations (Nair et al., 2006; Kgaswane et al., 2012), whereas the model which we use is free of these limitations (Youssof et al., 2013).

The sharpness of the Moho depends on (i) the contrast in velocity and density across the crust–mantle transition and (ii) the thickness of this transition. These parameters affect the amplitude and frequency of the converted Ps phase and its multiples: a sharp Moho is characterized by high amplitude and short duration of the signal, whereas a gradual Moho is characterized by small amplitude and long signal duration. An RF analysis of P to S conversions based on the full Hk-stacking interpretation of data recorded by all 82 broadband seismic stations of the SASE experiment allowed to constrain, for the first time, the map of the Moho "sharpness" (Youssof et al., 2013), defined by amplitude of the Pds-converted phase from the Moho.

The usual definition of sharpness in seismology is, however, related to the thickness of a gradational discontinuity (e.g. Vinnik, 1977). The amplitude of Pds depends on the true sharpness and on the S-wave velocity contrast at the discontinuity. To get a large reflected signal, the width h of a gradational discontinuity should be less than a quarter of the wavelength λ, $h < \lambda/4$ (Richards, 1972). If the amplitude of the phase reflected from a gradational boundary is inversely proportional to the travel-time difference Δ between the signals reflected from the top and bottom of the gradational boundary, then for vertical seismic wave propagation the travel-time difference should be less than half-period T, $\Delta < T/2$, to get a reflected signal. For the Pds transmitted phase, the signal from the bottom of the gradational boundary arrives later than the signal from the top boundary by time $[h/Vs - h/V_P]$, where V_P and V_S are P- and S-wave velocities. If one assumes $V_P/V_S = 1.8$ as a typical value for mantle rocks (Christensen, 1996), the rule of $h < \lambda/4$ for reflected phases transforms to $h < 1.1\,\lambda$ for the Pds-converted phases, where λ is wavelength of the S-wave.

For dominant periods of ca. 2 s used by Youssof et al. (2013), the amplitude of the Pds phase from the Moho is large, if the thickness of the Moho transition is less than 9 km. Much larger thickness is required for a significant reduction of the amplitude of Pds. This suggests that the "sharpness" defined by amplitude of the Pds-converted phase from the Moho is mainly an indicator of the S-wave velocity contrast at the Moho boundary, rather than the thickness of the gradational zone at the Moho boundary. We use here the quantitative measure of sharpness (Youssof et al., 2013) as the amplitude of the Ps phase for each stacked trace beneath a station, normalized by the average regional Ps amplitude (Fig. 9a).

A sharp Moho is typical of regions with a thin crust and relatively small Vp/Vs (most of the Archaean Zimbabwe and Kaapvaal cratons), whereas a gradual Moho is common in the Limpopo belt, the Namaqua–Natal Mobile belt, and in the Bushveld Intrusive Complex, where high Vp/Vs ratio is common (Youssof et al., 2013). Variability of the crustal-mantle transition may be related to magmatism and underplating as has been observed in sedimentary basins from controlled source seismology (Thybo et al., 1998; Jensen and Thybo, 2002).

A comparison of regional variations in the Moho sharpness in southern Africa (Fig. 9a) with the distribution of kimberlites (Fig. 9b) demonstrates that kimberlites tend to be in regions with a sharp Moho. A sharp Moho can be caused by the presence of a low-density, felsic, lower crust (James et al., 2003), and/or can result from delamination of the lower crust and the lithosphere mantle (Bird, 1979; Kay and Kay, 1993; Zegers and van Keken, 2001), as a result of gravitational instability associated with tectono-magmatic events (Menard and Molnar, 1988; Artemieva and Meissner, 2012). In such a case, the lithospheric mantle would be replaced by a new mantle material, which will be younger in age and more fertile. However, geochronological studies of crustal and mantle xenoliths from the Kaapvaal kimberlites indicate similar ages for the crust and the underlying lithospheric mantle (Pearson, 1999), particularly down to ca. 125 km depth (Fig. 10). Therefore, if the lower crust and the lithospheric mantle of the Kaapvaal craton were delaminated, this

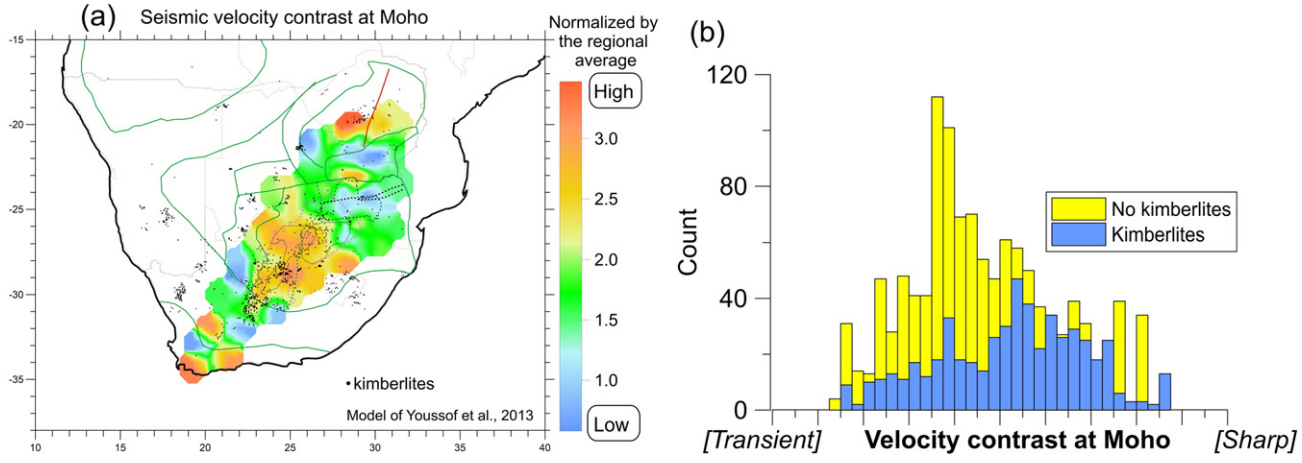

Fig. 9. (a) Map of Moho sharpness based on P–S receiver functions (Youssof et al., 2013). Moho sharpness is quantified by seismic velocity contrast at the Moho at each seismic station normalized by the average value for all SASE stations; dots—kimberlite pipes; (b) histograms of velocity contrast at Moho for regions with and without kimberlites (calculated on a 15 × 15 min grid for (a)).

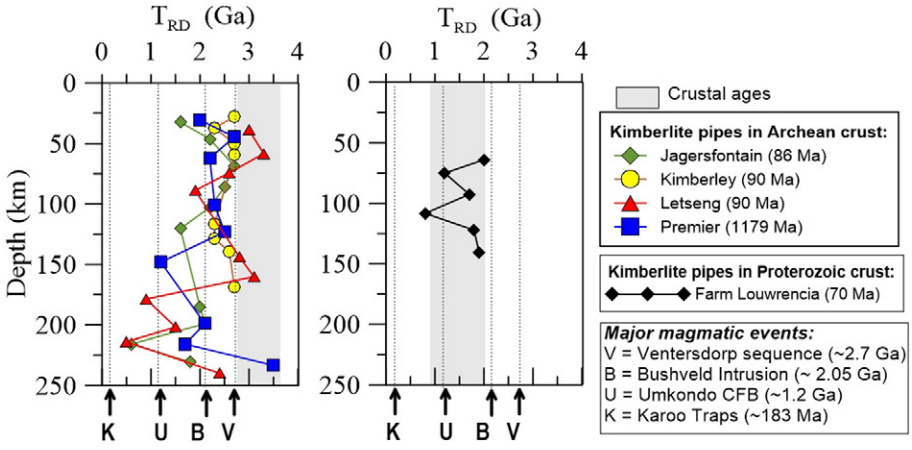

Fig. 10. Re–Os modal ages of the lithospheric mantle in southern Africa (based on data by Pearson, 1999).

process should have taken place already in late Archean–early Proterozoic, and in that case, it may have been related to the Ventersdorp magmatic event (Fig. 10).

Alternatively, blocks with a sharp Moho, low Vp/Vs crust, and depleted lithospheric mantle may represent ancient, weakly reworked Archean lithosphere (Fig. 11b). This interpretation is supported by an intriguing correlation between the Moho sharpness and the SPT density of the lithospheric mantle (Fig. 11a). Statistically, lithosphere blocks with sharp Moho (and numerous kimberlite pipes, Fig. 9a) have low-density lithospheric mantle, whereas blocks with gradual Moho have moderate-density mantle. In such a case, blocks with transitional Moho, high Vp/Vs crust, and moderate-density lithospheric mantle are areas that have been affected by a significant melt-metasomatism (leading to density increase in the sub-Moho lithosphere), with infiltration of basaltic magmas into the crust (leading to a high crustal Vp/Vs ratio), and basaltic underplating at around Moho (leading to the increase in crustal thickness with a transitional Moho) (Fig. 11b).

7. Mantle density versus Vp, Vs upper mantle velocities

We next compare mantle density structure at in situ conditions (Fig. 5a) to regional seismic velocity models (Figs. 12, 13) based on teleseismic traveltime tomographic inversion of the P- and S-body wave data recorded by the southern Africa seismic experiment (SASE) (Youssof et al., 2015; James et al., 2001). Both tomographic models are constrained with respect to similar continental reference models, ak135 and iaspei91, respectively. It is outside the scope of the present paper to discuss potential causes of the discrepancies between the two regional tomographic models (Foulger et al., 2013).

A visual comparison of the density structure of the lithospheric mantle in southern Africa with seismic velocities constrained by regional tomography models shows some correlation between density and velocity anomalies in the upper mantle at 100–150 km depth (Fig. 12). However, statistical analysis does not demonstrate any simple quantitative links between Vp, Vs, and mantle density. The absence of correlation between seismic velocities and density in peridotite-type rocks has been reported earlier based on studies of the Kaapvaal peridotites, which included laboratory measurements of elastic and thermal moduli on ca. 120 xenolith samples from the Kaapvaal and adjacent Proterozoic mobile belts (James et al., 2004). That study concluded that while seismic velocity variations in southern Africa are controlled primarily by temperatures, with weak compositional effects, density variations are controlled chiefly by compositional variations, with only a minor effect of temperature variation on density. Note that in our comparison of mantle density and mantle seismic velocity, the temperature effect is unimportant since we take both parameters at in situ conditions, and therefore it is primarily the composition of the lithospheric mantle that leads to non-unique correlations between seismic velocities and density (Figs. 12, 13). The lack of simple quantitative correlation

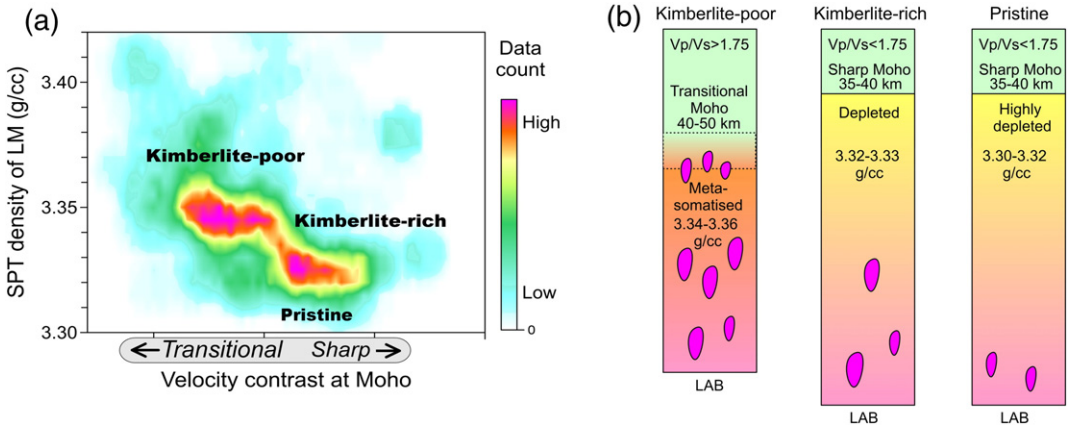

Fig. 11. (a) Correlation between the seismic velocity contrast at the Moho and SPT density of the lithospheric mantle (the case of 0.5 km dynamic topography, Fig. 2a); colors show density distribution of data points calculated on a 30 × 30 min grid. Data on the number of kimberlite pipes (kimberlite rich vs kimberlite poor) are based on Fig. 9b: data cluster with the transitional velocity contrast at the Moho and lithospheric mantle density of around 3.35 g/cm^3 corresponds to kimberlite-poor cells, while data cluster with a sharp Moho and lithospheric mantle density of 3.32–3.33 g/cm^3 corresponds to kimberlite-rich cells. "Pristine" mantle with low values of LM density and sharp Moho lacks kimberlites. (b) Conceptual model showing links between depth to the Moho, Moho sharpness, crustal Vp/Vs, mantle density, lithosphere thickness, and kimberlite occurrences.

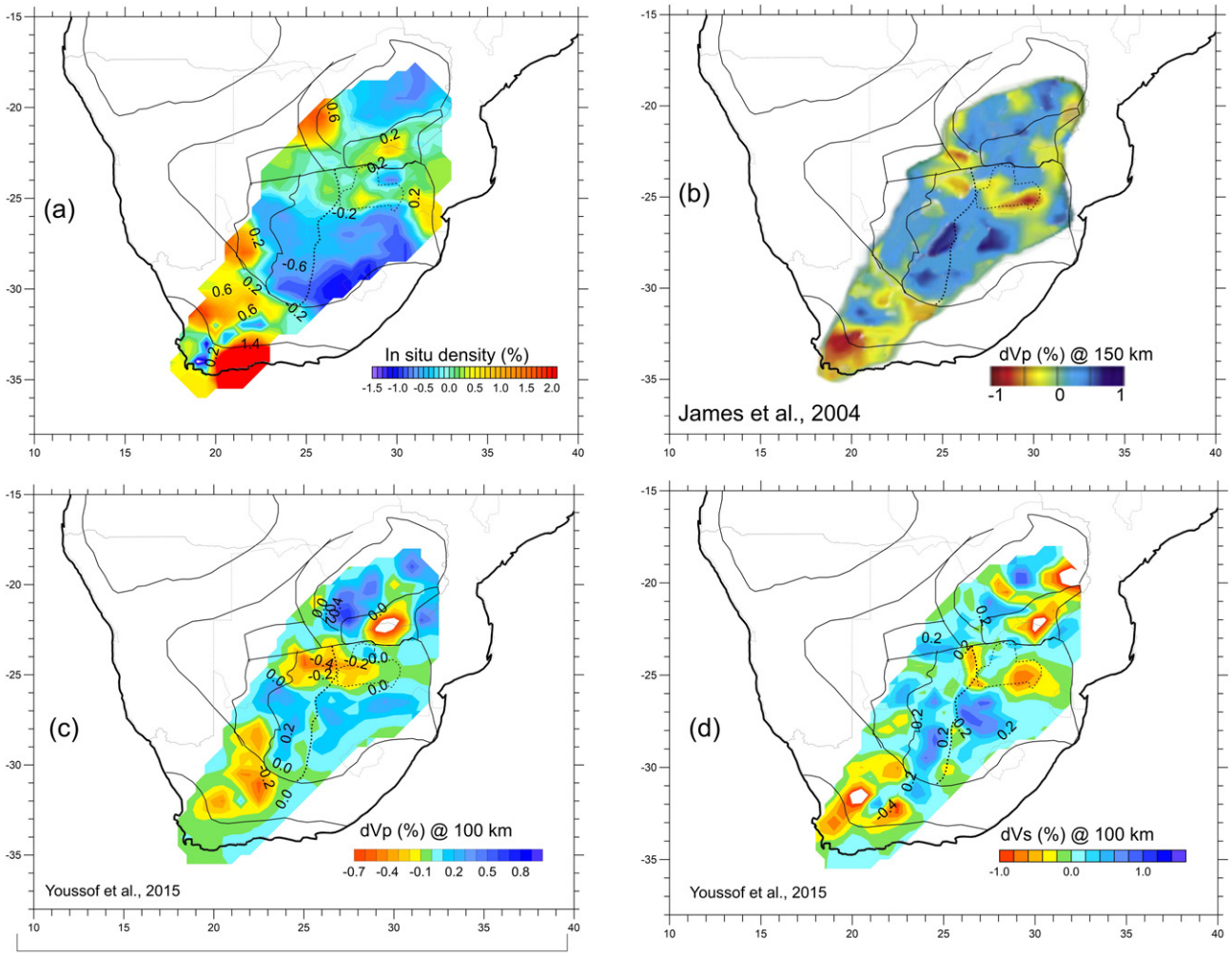

Fig. 12. Comparison of density of the lithospheric mantle at in situ conditions (Fig. 5a) with regional seismic tomography models. (a) In situ density anomalies in the lithospheric mantle as per cent of in situ asthenosphere density (3.23 g/cm^3); (b) Vp velocity anomaly at 150 km depth with respect to iaspei91 model (based on James et al., 2001); (c, d) Vp and Vs velocity anomalies at 100 km depth with respect to ak135 model (based on Youssof et al., 2015).

between seismic velocities and mantle density (Fig. 13a) may also be ascribed to a significantly different lateral resolution of seismic and density models, as well as to a significant uncertainty in seismic amplitudes (Foulger et al., 2013) and in the mantle density model (see details in Artemieva and Vinnik, 2016). To reduce the effect of model resolution and uncertainties in amplitudes, we averaged seismic Vp, Vs values and mantle density values for several tectonic blocks in Southern Africa (Fig. 13). The analysis performed this way indicates an inverse correlation between in situ density and in situ seismic velocities in the cratonic lithospheric mantle in southern Africa: tectonic blocks with high seismic velocities have low-density mantle, whereas reduced seismic velocities in the cratonic lithospheric mantle correspond to increased values of mantle density.

The observed trend is in agreement with a number of studies (Jordan, 1979; Jordan, 1988; Lee, 2003), which demonstrate that mantle rocks with high Mg# (typical of rocks depleted in basaltic components) have significantly lower densities and higher seismic velocities than fertile rocks. Importantly, both Vp and Vs correlate with mantle density only on a regional scale, with a large scatter observed for all tectonic blocks. In support of previous studies (James et al., 2004; O'Reilly and Griffin, 2006), it suggests complex, non-linear relationships between seismic velocities and densities in the cratonic mantle, which may not be parameterized by one parameter, such as Mg#, but require incorporation of data on other minerals, particularly garnet and orthopyroxene (Kopylova et al., 2004; Matsukage et al., 2005).

8. Conclusions

We present and discuss the new regional model for the depth-averaged density structure of the lithospheric mantle in southern Africa. The results demonstrate the following.

1) Density structure of the lithospheric mantle is highly heterogeneous laterally and it is well correlated with tectonic provinces and crustal ages. There is a general trend in a gradual increase in lithosphere mantle density from the Archean to Phanerozoic terranes, with density values in the range reported in petrological studies. Several terranes (the southern Kheis belt, the Limpopo belt, the Barberton greenstone belt/Swaziland, and the western part of the Zimbabwe craton) deviate from the general trend by a nearly constant value of mantle density anomaly of ca. 0.03 g/cm^3, which we attribute to melt-metasomatism with an addition of basaltic material.
We observe a significant small-scale density heterogeneity within tectonic blocks of the same ages. The Witwatersrand basin and the Bushveld intrusion appear as coherent blocks with increased lithosphere mantle density (3.34–3.35 g/cm^3) as compared to most of the Kaapvaal craton (3.31–3.34 g/cm^3). Mantle of the eastern Zimbabwe craton is low dense and similar to the Kaapvaal, while the western Zimbabwe has high-density (3.37–3.40 g/cm^3) mantle. The Eastern and Western provinces of the Cape Fold belt have significantly different mantle density structure (3.40–3.42 g/cm^3 and

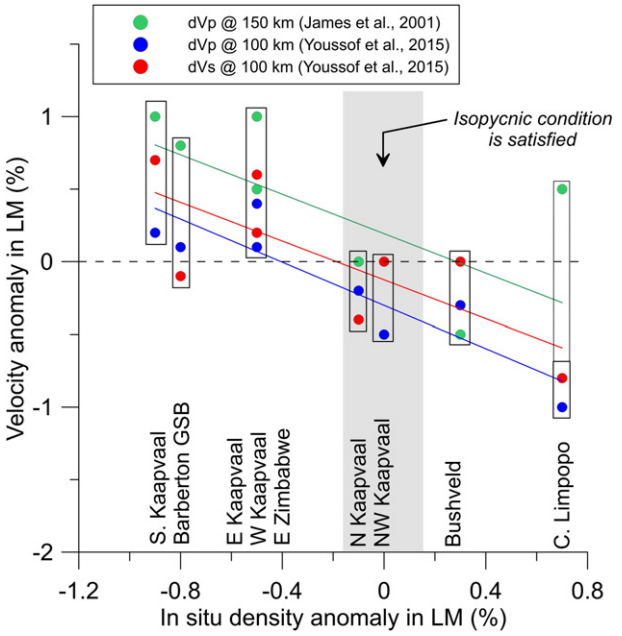

Fig. 13. Correlations between in situ density of the lithospheric mantle (Fig. 12a) and seismic velocity anomalies at 100 and 150 km depth (Fig. 12 bcd). Density values characteristic for different tectonic blocks in southern Africa provide averages for the entire thickness of the lithospheric mantle (from the Moho down to the LAB). Despite a significant scatter in data due to different vertical and lateral resolution of the compared models, there is a clear correlation between in situ density and in situ seismic velocities in the cratonic lithospheric mantle. Lines—best fit trends for different tomography models. Gray shading marks tectonic blocks where the isopycnic condition is satisfied.

3.3.4–3.37 g/cm^3, respectively): the Western province may include remnants of ancient cratonic lithosphere, while mantle of the Eastern province may host eclogite-rich oceanic slabs.

Isopycnicity condition is satisfied locally. For most of the Archean part deviations of bulk mantle density from the bulk isopycnicity are within the range of 0.01–0.02 g/cm^3, which is close to the model uncertainty. Post-Archean blocks and the Limpopo belt show large deviations from isopycnicity.

2) We analyze the pattern of kimberlite distribution with respect to the density structure of the lithospheric mantle. Most kimberlites are associated with depleted mantle (SPT density 3.32–3.33 g/cm^3). Single and scattered pipes within the Cape Fold belt and the Namaqua–Natal belt all fall onto the regions with depleted lithospheric mantle. The most depleted parts of the craton (density 3.30–3.31 g/cm^3) do not host kimberlites.

   Group I and Group II kimberlites of the Kaapvaal craton with the ages of <95 Ma and >110 Ma, correspondingly, are emplaced in the lithospheric mantle with different density (3.35 ± 0.03 g/cm^3 and 3.33 ± 0.01 g/cm^3), with older kimberlites sampling more depleted mantle. We speculate that age-dependent differences in mantle density reflect progressive metasomatic modification of cratonic mantle.

   Diamondiferous kimberlites are more common in regions with a lower density mantle (3.32–3.35 g/cm^3), while those which sample more dense mantle are older than 200 Ma. Non-diamondiferous kimberlites exist in mantle with a broad range of densities.

3) Our results demonstrate an amazing correlation between the Moho sharpness and the density of the lithospheric mantle. Lithosphere blocks with sharp Moho host numerous kimberlite pipes and have low-density lithospheric mantle, whereas blocks with gradual Moho have moderate-density mantle and are kimberlite poor. We attribute this pattern to (apparently, pre-kimberlite) melt-metasomatism which affected both the composition of the lithospheric mantle and the sharpness of Moho through magmatic underplating and intrusions, and made mantle rheology and composition unfavorable for kimberlite-type magmatism.

On a regional scale, mantle density structure correlates with seismic velocities in the upper mantle, with higher seismic velocities being observed in regions with lower mantle density. The correlation is, however, weak and indicates that velocity–density relationship in the lithospheric mantle is strongly non-unique.

Supplementary data to this article can be found online at http://dx.doi.org/10.1016/j.gr.2016.05.002.

Digital density model can be requested from the authors (irina@ign.ku.dk).

Acknowledgments

This study is supported by FNU grant DFF-1323-00053 to IMA. Stimulating discussions with Hans Thybo on the lithosphere structure in southern Africa are gratefully acknowledged. Constructive comments of two anonymous reviewers helped to improve clarity of the presentation.

References

Artemieva, I.M., Vinnik, L.P., 2016. Density structure of the cratonic mantle in southern Africa: 1. Implications for dynamic topography. Gondwana Research http://dx.doi.org/10.1016/j.gr.2016.03.002.

Artemieva I.M. and Meissner R., 2012. Crustal thickness controlled by plate tectonics: a review of crust–mantle interaction processes illustrated by European examples. Tectonophysics, v. 530-531, 18–49

Artemieva, I.M., Mooney, W.D., 2001. Thermal structure and evolution of Precambrian lithosphere: A global study. Journal of Geophysical Research 106, 16387–16414.

Artemieva, I.M., 2006. Global 1°×1° thermal model TC1 for the continental lithosphere: implications for lithosphere secular evolution. Tectonophys. 416, 245–277.

Artemieva, I.M., 2009. The continental lithosphere: reconciling thermal, seismic, and petrologic data. Lithos 109, 23–46.

Artemieva, I.M., 2007. Dynamic topography of the East European Craton: shedding light upon the lithospheric structure, composition and mantle dynamics. Global and Planetary Change 58, 411–434.

Artemieva, I.M., 2003. Lithospheric structure, composition, and thermal regime of the East European craton: implications for the subsidence of the Russian Platform. Earth and Planetary Science Letters 213, 429–444.

Bailey, D.K., 1982. Mantle metasomatism. Nature 296, 525–530.

Barth, M.G., Rudnick, R.L., Horn, I., McDonough, W.F., Spicuzza, M.J., Valley, J.W., Haggerty, S.E., 2001. Geochemistry of xenolithic eclogites from West Africa, part I: a link between low MgO eclogites and Archean crust formation. Geochimica et Cosmochimica Acta 65 (9), 1499–1527.

Bird, P., 1979. Continental delamination and the Colorado Plateau. Journal of Geophysical Research 84, 7561–7571.

Boyd, F.R., 1989. Compositional distinction between oceanic and cratonic lithosphere. Earth and Planetary Science Letters 96, 15–26.

Brocker, T., 2005. Empirical relations between elastic wavespeeds and density in the earth's crust. Bull. Seism. Soc. Am. 95, 2081–2092.

Campbell, I.H., Naldrett, A.J., and Barnes, S.J., 1983. A model for the origin of the platinum-rich sulfide horizons in the Bushveld and Stillwater complexes:J. Petrology, 24, 133–165.

Carlson, R.W., Pearson, D.G., Boyd, F.R., Shirey, S.B., Irvine, G.J., Menzies, A.H., Gurney, J.J., 1999. Re–Os systematics of lithospheric peridotites: implications for lithosphere formation and preservation. In: Gurney, J.J., Gurney, J.L., Pascoe, M.D., Richardson, S.H. (Eds.), Proc. 7th Intern. Kimberlite Conf., Cape Town, v. 1, The J. B. Dawson Volume. Red Roof Design, Cape Town, pp. 99–108.

Carlson, R.W., Irving, A., Schultze, D., Hearn, B., 2004. Timing of Precambrian melt depletion and Phanerozoic refertilization events in the lithospheric mantle of the Wyoming Craton and adjacent Central Plains Orogen. Lithos 77, 453–472.

Carlson, R.W., Pearson, G., James, D.E., 2005. Physical, chemical, and chronological characteristics of continental mantle. Reviews of Geophysics 43 (1–24), RG1001. http://dx.doi.org/10.1029/2004RG000156.

Cherepanova, Y., Artemieva, I.M., 2015. Density heterogeneity of cratonic lithospheric mantle: a case study of the Siberian craton. Gondwana Research 28 (4), 1344–1360.

Christensen, N.I., 1979. Compressional wave velocities in rocks at high temperatures and pressures, critical thermal gradients, and crustal low-velocity zones. Journal of Geophysical Research 84, 6849–6857.

Christensen, N.I., 1996. oisson's ratio and crustal seismology. J. Geophys. Res.m 101, 3139–3156.

Clifford, T.N., 1966. Tectono-metallogenic units and metallogenic provinces of Africa. Earth and Planetary Science Letters 1, 421–434.

Coltorti, M. and Gregoire M. (eds.), 2008. Metasomatism in Oceanic and Continental Lithospheric Mantle. Geol. Soc. London, Sp. Publ., 293, isbn 978–1–86239-242-7.

Cordier, C., Sauzeat, L., Arndt, N.T., et al., 2015. Metasomatism of the lithospheric mantle immediately precedes kimberlite eruption: new evidence from olivine composition and microstructures. J. Petrology 56, 1775–1796.
de Wit, M.J., Roering, C., Hart, R.J., Armstrong, R.A., de Ronde, C.E.J., Green, R.W.E., Tredoeaux, M., Pederby, E., Hart, R.A., 1992. Formation of an Archaean continent. Nature 357, 553–562.
Eaton, D.W., Perry, H.K.C., 2013. Ephemeral isopycnicity of cratonic mantle keels. Nature Geoscience 6, 967–970.
Faure, S., 2006. World Kimberlites and Lamproites CONSOREM Database (Version 2006–1). Consortium de Recherché en Exploration Minarale CONSOREM, Université du Quebec á Montreal, Numerical Database (www.consorem.ca).
Foulger, et al., 2013. Caveats on tomographic images. Terra Nova 0 (0), 1–23.
Gaul, O.F., Griffin, W.L., O'Reilly, S.Y., Pearson, N.J., 2000. Mapping olivine composition in the lithospheric mantle. Earth and Planetary Science Letters 182, 223–235.
Goodwin, A.M., 1996. Principles of Precambrian geology. Academic Press, London, San Diego, Toronto (327 pp.).
Griffin, W.L., O'Reilly, S.Y., Natapov, L., Ryan, C., 2003. The evolution of lithospheric mantle beneath the Kalahari Craton and its margins. Lithos 71, 215–241.
Gurney, J.J., 1984. A correlation between garnets and diamonds. In: Glover, J.E., Harris, P.G. (Eds.), Kimberlite Occurrence and Origin: A Basis for Conceptual Models in Exploration. Geology Department and University Extension, University of Western Australia Publication Vol. 8, pp. 143–166.
Hanson, R.E., Crowley, J.L., Bowring, S.A., Ramezani, J., Gose, W.A., Dalziel, I.W.D., Pancake, J.A., Seidel, E.K., Blenkinsop, T.G., Mukwakwami, J., 2004. Coeval large scale magmatism in the Kalahari and Laurentian cratons during Rodinia assembly. Science 304, 1126–1129.
Hawkesworth, C.J., Kempton, P.D., Rogers, N.W., Ellam, R.M., van Calsteren, P.W., 1990. Continental mantle lithosphere, and shallow level enrichment process in the Earth's mantle. Earth Plan. Sci. Lett. 96, 256–268.
Herceg, M., Artemieva, I.M., Thybo, H., 2016. Sensitivity analysis of crustal correction for calculation of lithospheric mantle density from gravity data. Geophysical Journal International 204, 738–747.
Ionov, D.A., Doucet, L.S., Carlson, R.W., Golovin, A.V., Korsakov, A.V., 2015. Post-Archean formation of the lithospheric mantle in the central Siberian craton: Re–Os and PGE study of peridotite xenoliths from the Udachnaya kimberlite. Geochimica et Cosmochimica Acta 165, 466–483.
Irvine, G.I., Pearson, D.G., Carlson, R.W., 2001. Lithospheric mantle evolution in the Kaapvaal craton: a Re–Os isotope study of peridotite xenoliths from Lesotho kimberlites. Geophysical Research Letters 28, 2505–2508.
James, D.E., Fouch, M.J., VanDecar, J.C., van der Lee, S., Kaapvaal Seismic Group, 2001. Tectospheric structure beneath southern Africa. Geophysical Research Letters 28, 2485–2488.
James, D., Niu, F., Rokosky, J., 2003. Crustal structure of the Kaapvaal Craton and its significance for early crustal evolution. Lithos 71, 413–429.
James, D.E., Boyd, F.R., Schutt, D., Bell, D.R., Carlson, R.W., 2004. Xenolith constraints on seismic velocities in the upper mantle beneath southern Africa. Geochemistry, Geophysics, Geosystems 5 (1), Q01002. http://dx.doi.org/10.1029/2003GC000551.
Janse, A.J.A., 1991. Is Clifford's rule still valid? Affirmative examples from around the world. 5th International Kimberlite Conference, Araxa, Brazil. Extended Abstracts, pp. 196–198.
Jensen, S.L., Thybo, H., 2002. Moho topography and lower crustal wide-angle reflectivity around the TESZ in southern Scandinavia and northeastern Europe. Tectonophysics 360, 187–213.
Jerde, E.A., Taylor, L.A., Crozaz, G., Sobolev, N.V., Sobolev, V.N., 1993. Diamondiferous eclogites from Yakutia, Siberia—evidence for a diversity of protoliths. Contributions to Mineralogy and Petrology 114 (2), 189–20.2.
Jones, A.G., Evans, R.L., Muller, M.R., et al., 2009. Area selection for diamonds using magnetotellurics: examples from southern Africa. Lithos 112, 83–92.
Jordan, T.H., 1975. The continental tectosphere. Reviews of Geophysics and Space Physics 13, 1–12.
Jordan, T.H., 1978. Composition and development of the continental tectosphere. Nature 274, 544–548.
Jordan, T.H., 1979. Mineralogies, densities and seismic velocities of garnet lherzolites and their geophysical implications. In: Boyd, F.R., Meyer, H.O.A. (Eds.), The mantle sample: Inclusions in kimberlite and other volcanics. American Geophysical Union, Washington, D.C., pp. 1–14.
Jordan, T.H., 1988. Structure and formation of the continental tectosphere. J. Petrol. Special lithosphere issue 11–37.
Kaban, M.K., Schwintzer, P., Artemieva, I.M., Mooney, W.D., 2003. Density of continental roots: compositional and thermal effects. Earth and Planetary Science Letters 209, 53–69.
Kay, R.W., Kay, S., 1993. Delamination and delamination magmatism. Tectonophysics 219, 177–189.
Kelly, R.K., Kelemen, P.B., Jull, M., 2003. Buoyancy of the continental upper mantle. Geochemistry, Geophysics, Geosystems 4 (2), 1017. http://dx.doi.org/10.1029/2002GC000399.
Kennedy, C.S., Kennedy, G.C., 1976. The equilibrium boundary between graphite and diamond. Journal of Geophysical Research 81, 2467–2470.
Kennett, B., Furumura, T., 2016. Multiscale seismic heterogeneity in the continental lithosphere. Geochemistry, Geophysics, Geosystems http://dx.doi.org/10.1002/2015GC006200.
Kgaswane, E.M., Nyblade, A.A., Durrheim, R.J., et al., 2012. Shear wave velocity structure of the Bushveld Complex, South Africa. Tectonophysics 554, 83–104.
Kopylova, M.G., Gurney, J.J., Daniels, L.R.M., 1997. Mineral inclusions in diamonds from the River Ranch kimberlite, Zimbabwe. Contributions to Mineralogy and Petrology 129, 366–384.
Kopylova, M.G., Lo, J., Christensen, N.I., 2004. Petrological constraints on seismic properties of the Slave upper mantle (Northern Canada). Lithos 77, 493–510.
Kopylova, M.G., Beausoleil, Y., Goncharov, A., Burgess, J., Strand, P., 2016. Spatial distribution of eclogite in the Slave cratonic mantle: the role of subduction. Tectonophysics 672-673, 87–103.
Kuskov, O.L., Kronrod, V.A., Annersten, H., 2006. Inferring upper-mantle temperatures from seismic and geochemical constraints: implications for Kaapvaal craton. Earth and Planetary Science Letters 244, 133–154.
Lebedev, S., Boonen, J., Trampert, J., 2009. Seismic structure of Precambrian lithosphere: new constraints from broad-band surface-wave dispersion. Lithosphere 109, 96–111. http://dx.doi.org/10.1016/j.lithos.2008.06.010.
Lee, C.-T.A., 2003. Compositional variation of density and seismic velocities in natural peridotites at STP conditions: implications for seismic imaging of compositional heterogeneities in the upper mantle. Journal of Geophysical Research 108 (B9), 2441. http://dx.doi.org/10.1029/2003JB002413.
Lekic, V., Romanowicz, B., 2011. Inferring upper-mantle structure by full waveform tomography with the spectral element method. Geoph. J. Int. 185, 799–831.
Mathez, E.A., 1995. Magmatic metasomatism and formation of the Merensky Reef, Bushveld Complex. Contributions to Mineralogy and Petrology 119 (2), 277–286.
Matsukage, K.N., Nishihara, Y., Karato, S.-I., 2005. Seismological signature of chemical differentiation of Earth's upper mantle. Journal of Geophysical Research 110, B12305. http://dx.doi.org/10.1029/2004JB003504 (18 pp.).
Menard, G., Molnar, P., 1988. Collapse of a Hercynian Tibetan plateau into a late Paleozoic European Basin and range province. Nature 334, 235–237.
Mitchell, R.H., 1995. Kimberlites, Orangeites, and Related Rocks. Plenum Press, New York.
Nair, S.K., Gao, S.S., Liu, K.H., Silver, P.G., 2006. Southern African crustal evolution and composition: constraints from receiver function studies. Journal of Geophysical Research 111, B02304.
Nataf, H.-C., Ricard, Y., 1996. 3SMAC: An a priori tomographic model of the upper mantle based on geophysical modeling. Physics of the Earth and Planetary Interiors 95, 101–122.
Neal, C.R., Taylor, L.A., Davidson, J.P., Holden, P., Halliday, A.N., Nixon, P.H., Paces, J.B., Clayton, R.N., Mayeda, T.K., 1990. Eclogites with oceanic crustal and mantle signatures from the Bellsbank kimberlite, South Africa, 2. Sr, Nd, and O isotope geochemistry. Earth and Planetary Science Letters 99 (4), 362–379.
Nguuri, T., et al., 2001. Crustal structure beneath southern Africa and its implications for the formation and evolution of the Kaapvaal and Zimbabwe Cratons. Geophysical Research Letters 28 (13), 2501–2504.
Niu, F., James, D.E., 2002. Constraints on the formation and composition of crust beneath the Kaapvaal craton from Moho reverberations. Earth and Planetary Science Letters 200, 121–130.
O'Reilly, S.Y., Griffin, W.L., 2006. Imaging global chemical and thermal heterogeneity in the subcontinental lithospheric mantle with garnets and xenoliths: geophysical implications. Tectonophysics 416, 289–309.
Pearson, D.G., Carlson, R.W., Shirey, S.B., Boyd, F.R., Nixon, P.H., 1995. Stabilisation of Archaean lithospheric mantle; a Re–Os isotope study of peridotite xenoliths from the Kaapvaal Craton. Earth and Planetary Science Letters 134, 341–357.
Pearson, D.G., 1999. The age of continental roots. Lithos 48, 171–194.
Poudjom Djomani, Y.H., O'Reilly, S.Y., Griffin, W.L., Morgan, P., 2001. The density structure of subcontinental lithosphere through time. Earth and Planetary Science Letters 184, 605–621.
Richards, P.G., 1972. Seismic waves reflected from velocity gradient anomalies within the Earth's upper mantle. Zeitschrift für Geophysik 38, 517–527.
Riley, T.R., Curtis, M.L., Leat, P.T., et al., 2006. Overlap of Karoo and Ferrar magma types in KwaZulu-Natal, South Africa. J. PETROLOGY 47, 541–566.
Saygin, E., Kennett, B., 2010. Ambient seismic noise tomography of Australian continent. Tectonophys. 481, 116–125.
Schmitz, M.D., Bowring, S.A., 2003. Ultrahigh-temperature metamorphism in the lower crust during Neoarchean Ventersdorp rifting and magmatism, Kaapvaal Craton, southern Africa. GSA Bulletin 115, 533–548. http://dx.doi.org/10.1130/0016-7606(2003)115.
Schultze, D., Coopersmith, H., Harte, B., Pizzolato, L.A., 2008. Mineral inclusions in diamonds from the Kelsey Lake Mine, Colorado, USA: depleted Archean mantle beneath the Proterozoic Yavapai province. Geochimica et Cosmochimica Acta 72, 1685–1695.
Scoon, R.N., 1987. Metasomatism of cumulus magnesian olivine by iron-rich postcumulus liquids in the upper Critical Zone of the Bushveld Complex. Mineralog. mag. 51, 389–396.
Shankland, T.J., Duba, A., 1990. Standard electrical conductivity of isotropic, homogeneous olivine in the temperature range 1200–1500 °C. Geophysical Journal International 103, 25–31.
Smith, C.B., 1983. Lead, strontium, and neodymium isotopic evidence for sources of African Cretaceous kimberlite. Nature 304, 51–54.
Smith, C.B., Pearson, D.G., Bulanova, G.P., et al., 2009. Extremely depleted lithospheric mantle and diamonds beneath the southern Zimbabwe Craton. Lithos 112, 1120–1132.
Snyder, D.B., Rondenay, S., Bostock, M.G., Lockhart, G.D., 2004. Mapping the mantle lithosphere for diamond potential using teleseismic methods. Lithos 77, 859–872.
Sobolev, N.V., 1974. Deep seated inclusions in kimberlites and the problem of the composition of the upper mantle. Nauka, Moscow (in Russian). English translation by D. A. Brown. AGU, Washington, D.C. (279 pp., 1977).
Stiefenhofer, J., Viljoen, K.S., Tainton, K.M., Dobbe, R., Hannweg, G.W., 1999. The Petrology of a mantle xenoliths suite from Venetia, South Africa. In: Gurney, J.J., Gurney, J.L., Pascoe, M.D., Richardson, S.H. (Eds.), Proc. 7th Intern. Kimberlite Conf., Cape Town, 1998, P.H. Nixon Volume 2, Red Roof Design, Cape Town, pp. 836–845.
Thybo, H., Perchuc, E., Gregersen, S., 1998. Interpretation in statu nascendi of seismic wide-angle reflections based on EUGENO-S data. Tectonophysics 289, 281–294.

Ulmer, P., Sweeney, R.J., 2002. Generation and differentiation of group II kimberlites: constraints from a high-pressure experimental study to 10 GPa. Geochimica et Cosmochimica Acta 66, 2139–2153.
Vinnik, L.P., 1977. Detection of waves converted from P to SV in the mantle. Physics of the Earth and Planetary Interiors 15, 39–45.
Walter, M.J., 1999. Melting residues of fertile peridotite and the origin of cratonic lithosphere. In: Fei, Y., Bertka, C.M., Mysen, B.O. (Eds.), Mantle Petrology: Field Observations and High Pressure Experimentation: A Tribute to Francis R. (Joe) Boyd. Geochem. Soc. Spec. Publ. No. 6, pp. 225–239.
Walter, M.J., 2005. Melt extraction and compositional variability in mantle lithosphere. In: Carlson, R.W. (Ed.), Treatise on Geochemistry Vol. V.2. Elsevier, Amsterdam, pp. 363–394.
Youssof, M., Thybo, H., Artemieva, I., Levander, A., 2015. Upper mantle structure beneath southern African cratons from seismic finite-frequency P- and S-wave tomography. Earth and Planetary Science Letters 420, 174–176.
Youssof, M., Thybo, H., Artemieva, I.M., Levander, A., 2013. Moho depth and crustal composition in southern Africa. Tectonophysics 609, 267–287.
Zegers, T.E., van Keken, P.E., 2001. Middle Archean continent formation by crustal delamination. Geology 29, 1083–1086.